Journal of Hazardous Materials 180 (2010) 375–383

Contents lists available at ScienceDirect

Journal of Hazardous Materials

journal homepage: www.elsevier.com/locate/jhazmat

Effects of nano-sized silicon dioxide on the structures and activities of three functional proteins

Zhen Xu[a], Shi-Long Wang[b], Hong-Wen Gao[a,*]

[a] State Key Laboratory of Pollution Control and Resource Reuse, College of Environmental Science and Engineering, Tongji University, Shanghai 200092, China
[b] School of Life Science and Technology, Tongji University, Shanghai 200092, China

ARTICLE INFO

Article history:
Received 23 December 2009
Received in revised form 12 April 2010
Accepted 12 April 2010
Available online 24 April 2010

Keywords:
Silica
Protein
Nanoparticles
Surface adsorption
Molecular interaction

ABSTRACT

Nanomaterials are finding increasing use in industrial production and daily life. However, human exposure to them may cause health risks. Nano-SiO_2 was selected as a representative nanomaterial and its potential effects were investigated in terms of its interactions with cytochrome *c* (cyt *c*), deoxyribonuclease (DNase II) and hemoglobin (Hb). The interactions accorded with Langmuir isothermal adsorption; the saturation binding numbers for cyt *c*, DNase II and Hb were 42 ± 5, 24 ± 2 and 1.1 ± 0.1 μmol/g nano-SiO_2 particle at pH 7.4, respectively, and the corresponding stability constants were 6.15×105, 1.79×106 and $2.6 \times 107\ M^{-1}$. On the basis of the binding constants and of ζ-potential fluorescence and circular dichroism (CD) measurements and scanning electronic microscopy (SEM), it was found that the three functional proteins can bridge nano-SiO_2 particles via charge attraction and hydrogen bonding and aggregate them into coralloid forms. The interactions also changed the secondary structures of the proteins and inhibited their static and dynamic activities. It may reasonably be deduced that exposure to nano-size silicon dioxide particles e.g. as drug carriers may have an unfavorable effect on human health by inactivating functional proteins.

1. Introduction

Recently, there has been increasing interest in the use of nanomaterials in industrial production and daily life; they have distinctive characteristics including high conductivity, strength, durability, and chemical reactivity, so they find applications in many fields [1–6]. These materials are increasingly being used commercially as fillers, opacifiers, catalysts, semiconductors, cosmetics, microelectronics and drug carriers [1,7]. It is therefore possible that human bodies will be exposed to nanomaterials, so it is important to consider the risks entailed. Nanomaterial particles are smaller than cells and cellular organelles, so they may penetrate these basic constructs and produce physical damage, inducing a harmful inflammatory response. Oxidative stress caused by nano-sized particles can damage lipids, carbohydrates, proteins and DNA; in particular, lipid peroxidation is considered most dangerous as it alters cell membrane properties [8–10]. Many epidemiological and experimental studies have indicated that ultrafine particles are closely associated with respiratory and cardiovascular diseases such as pneumonia, lung cancer, arteriosclerosis and myocardial infarction [11]. Recent studies have shown that nanomaterials can be genotoxic and cytotoxic in cultured human cells. There is evidence that nano-SiO_2 can cause inflammation, fibrosis, pulmonary damage and even DNA damage [12–14]. As an example, the cytotoxicity of silica nanoparticles was investigated in cultured human bronchoalveolar carcinoma-derived cells. Cell viability decreased significantly as a function of nanoparticle size. Exposure to SiO_2 nanoparticles increased reactive oxygen species (ROS) levels and reduced glutathione levels. Increased malondialdehyde production and lactate dehydrogenase release from the cells indicated lipid peroxidation and membrane damage [15].

Cytochrome *c* (Cyt *c*) occurs in plants, animals, and many unicellular organisms. Cyt *c* is a photoactive protein which mediates different biological process, such as the one present in apoptosis, a controlled process to destroy cells with DNA damage. Cyt *c* is also responsible for increasing cellular regeneration when red light is used in phototherapy. This molecule is the protein responsible for electron transfer in the cells mitochondria, being important for the energy transfer process in cells. The photoactive charge transfer in the cytochrome complex is attributed to the presence of a heme group linked to polypeptide chains [16,17]. It has been reported that the reaction of hydrogen peroxide with heme proteins, such as cyt *c*, produces highly reactive ferryl-heme species that are capable of oxidizing biomolecules and initiating lipid peroxidation [18,19]. The acid hydrolase deoxyribonuclease II (DNase II) is found in wide variety of animal tissues; its main subcellular location is in the lysosomes [20,21]. DNase II is a noncovalently linked azb heterodimer [22]. It is a well-characterized acid endonuclease that catalyzes

* Corresponding author. Tel.: +86 21 6598 8598; fax: +86 21 6598 8598.
E-mail address: hwgao@tongji.edu.cn (H.-W. Gao).

0304-3894/$ – see front matter © 2010 Elsevier B.V. All rights reserved.
doi:10.1016/j.jhazmat.2010.04.042

the hydrolysis of DNA into 3′-phosphoryl oligonucleotides in the absence of divalent metal ions [23]. Although its physiological significance is not yet fully understood, it is assumed to be important in DNA catabolism and fragmentation during apoptosis. Hemoglobin (Hb) is the iron-containing oxygen-transport metalloprotein in the red blood cells. As a carrier of oxygen, Hb transports oxygen from the lungs or gills to the rest of the body where it releases the oxygen for cell use. It also aids, both directly and indirectly, in carbon dioxide transport and regulates blood pH [24].

The interactions of nanomaterials (often nano-TiO_2 or nano-SiO_2) with functional biomolecules such as proteins, enzymes and DNA are regarded as preconditions for their cytotoxicity and organ toxicity. Various proteins have been investigated during recent years in this regard, e.g. fibrinogen, human serum albumin and lysine [25–27]. For example, Larsericsdotter reported electrostatic effects on protein adsorption using differential scanning calorimetry and adsorption isotherms [28]. Norde's measurements indicate that the structural perturbations induced by the hydrophilic silica surface are reversible, and irreversible surface-induced conformational changes may be related to the aggregation of BSA molecules after exposure to a hydrophobic surface [26]. Horie's investigation showed that the adsorption capacity of metal oxide nanoparticles is important for estimating the cytotoxicity of low-toxicity materials in vitro [29]. Nezu et al. reported that electrostatic interaction is the main mechanism controlling the adsorption of lysozyme to SiO_2 [30]. In this work, we studied the interactions of nano-SiO_2 with cyt *c*, DNase II and Hb. The objective was to identify the binding sites and types, estimate the effects on protein structure and activity, and elucidate the molecular toxicology.

2. Materials and methods

2.1. Instruments and materials

The absorption spectra of all suspensions/solutions were recorded with a Model Lambda-25 spectrometer (PerkinElmer, USA, wavelength range: 190–1100 nm, accuracy: ±0.1 nm, absorbance range: −3 to 4 A) equipped with a thermostatic cell holder to link with a Model TS-030 water-circulated thermostatic oven (Yiheng Sci. Technol. Shanghai, China). A Model J-715 circular dichroism (CD) Spectropolarimeter (Jasco Instrum., Japan, wavelength range: 165–900 nm) was used to measure protein conformations. Fluorescence spectra were recorded with a Model F-4500 Fluorescence Spectrophotometer (Hitachi, Japan, wavelength range: 200–900 nm, wavelength accuracy: ±2.0 nm, resolution: 1.0 nm). ζ-potentials were measured with a Model Zetasizer Nano ζ-Potential Analyzer (Malvern Instruments, UK, motion range: ±10 μcm/Vs, conductivity range: 0–200 mS/cm, minimum volume: 0.75 mL, temperature: 2–90 °C). A Model LS230 Particle Size Analyzer (Beckman Coulter, USA, diffraction illuminating source: solid state (780 nm), particle size analysis range: 0.04–2000 μm) with a Model LFC-101 Laser Channel (Ankersmid Ltd., Holland) was used to measure the size distribution of the aggregated particles. A scanning electron microscope (SEM) (Model Quanta 200 FEG, FEI Co., USA, accelerating voltage: 200 V to 30 kV) was used to measure the sizes and shapes of the nano-SiO_2 and nano-SiO_2-protein particles. A Model TG16-WS centrifuge (Hunan Xiangyi Instruments, China, max speed: 16000 rpm, max RCF 17800 × *g*, max Capacity 12 × 10 ml, speed accuracy ±50 rpm) was used to separate the particles.

Nano-SiO_2 (2.00 mg/L) (Aerosil 200, Degussa, average particle size 12 nm, purity > 99.8%, Germany) was used without further modification. It was suspended in deionized water and mixed ultrasonically for 10 min before use. Cyt *c* from horse heart (2.00 mg/mL) (purity > 95%, Sigma, USA) and DNase II from porcine spleen (2.00 mg/mL) (BR, 2000–6000 Kunitz units/mg protein (biuret), Shanghai Kayon Biological Technology, China) were freshly prepared. Hb from bovine blood (2.00 mg/mL) ($N \geq 15\%$, Shanghai Chemical Reagents, China Med. Group) was dissolved in deionized water and stored at less than 4 °C. Britton–Robinson (B–R) buffers, from pH 4.0 to 8.4, were prepared to adjust the acidities of solutions, and the ionic strengths were adjusted with 1.5 M NaCl. DNA (Purity ≥ 85%, storage temp.: 4 °C), agarose and other regular reagents were purchased from China Med. Group. Methyl green was obtained from Shanghai Kayon Biological Technology (China, Dye Content: >65%).

2.2. Photometric determination of nano-SiO_2–protein interactions [31]

Proteins and SiO_2 were mixed in 10-mL calibrated flasks containing 6.25–300 mg/L cyt *c* and 150 mg/L nano-SiO_2 particles, 6.25–850 mg/L DNase II and 300 mg/L nano-SiO_2 particles or 6.25–450 mg/L Hb and 300 mg/L nano-SiO_2 particles; 2.0 mL pH 7.4 B–R buffer and 1.0 mL 1.5 M NaCl were added. Each suspension was diluted to 10.0 mL with deionized water and mixed thoroughly. The calibrated flasks were incubated in a water bath at 37 °C with magnetic stirring (500 rpm). After 24 h, the solids with adsorbed proteins were separated by centrifugation at 12,000 rpm for 10 min. The absorbances of the supernatants containing cyt *c* and Hb were measured at 405 nm by UV–vis spectrophotometry and those with DNase II at 280 nm. A reagent blank without cyt *c*, Hb or DNase II was prepared simultaneously by the same procedures.

Using these procedures, a series of suspensions were prepared, initially containing 0, 50, 100, 150, 200, 250 and 300 mg/L cyt *c*, 150 mg/L nano-SiO_2, 2.0 mL pH 7.4 B–R buffer and 1.0 mL 1.5 M NaCl. Two other series of suspensions were prepared, initially containing (a) 0, 100, 300, 500, 700, 800 and 850 mg/L DNase II, 300 mg/L nano-SiO_2, 2.0 mL pH 7.4 B–R buffer and 1.0 mL 1.5 M NaCl, and (b) 0, 75, 150, 225, 300, 375 and 450 mg/L Hb, 300 mg/L nano-SiO_2, 2.0 mL pH 7.4 B–R buffer and 1.0 mL 1.5 M NaCl. Each suspension was diluted to 10.0 mL with deionized water and mixed thoroughly. The calibrated flasks were incubated in a water bath for 24 h at 37 °C with magnetic stirring (500 rpm). After 24 h the absorption spectra of the suspensions were measured between 480 and 600 nm against water.

2.3. Particle size and ζ-potential measurement [32]

The same procedures were used to prepare three series of suspensions initially containing 0–300 mg/L cyt *c* and 150 mg/L nano-SiO_2 particles, 0–850 mg/L DNase II and 300 mg/L nano-SiO_2 particles and 0–450 mg/L Hb and 300 mg/L nano-SiO_2 particles, all containing 2.0 mL pH 7.4 B–R buffer and 1.0 mL 1.5 M NaCl. Each suspension was diluted to 10.0 mL with deionized water and mixed thoroughly. The calibrated flasks were incubated in a water bath for 24 h at 37 °C with magnetic stirring at 500 rpm. The size distribution of the particles in suspension was measured using a particle size analyzer, and their ζ-potentials were measured with a ζ-potential analyzer.

2.4. Fluorescence measurement [33]

The following suspensions were prepared in 10-mL calibrated flasks: 75 mg/L cyt *c* and 0–900 mg/L nano-SiO_2 particles, 350 mg/L DNase II and 0–400 mg/L nano-SiO_2 particles and 100 mg/L Hb and 0–500 mg/L nano-SiO_2 particles. All the suspensions contained 2.0 mL pH 7.4 B–R buffer and 1.0 mL 1.5 M NaCl. They were diluted to 10.0 mL with deionized water and mixed thoroughly. After 10 min, the fluorescence spectrum of each suspension was measured with excitation wavelength 280 nm and emission wave-

length between 290 and 380 nm (both 5 nm slit widths). The solids with adsorbed proteins were separated by the aforementioned method and the fluorescence spectra of the supernatants were obtained. Simultaneously, a reagent blank without proteins was performed by the same procedure.

2.5. CD measurement [34]

CD spectra were recorded over the range 190–250 nm at 37 °C using a spectropolarimeter. Seventy-five milligrams per litre cyt *c* was mixed with 0, 100, 200, and 300 mg/L nano-SiO_2 particles, 150 mg/L DNase II with 0, 150, 300, and 500 mg/L nano-SiO_2 particles, and 100 mg/L Hb with 0, 100, 200, and 300 mg/L nano-SiO_2 particles. All the suspensions contained 1 mL pH 7.4 B–R buffer and each was diluted to 10 mL. The suspensions were incubated in a water bath at 37 °C with magnetic stirring at 500 rpm. After 24 h, CD spectra were obtained using a 0.1-cm light path cell. The mean residue ellipticity (MRE) was calculated and corrected with a reagent blank without proteins. Three replicate measurements were made on each suspension. The relative contents of α-helix, β-pleated sheet, β-turn and random coil were calculated.

2.6. Peroxidase activity of cytochrome c and activity of deoxyribonuclease II

The peroxidase activity of cyt *c* was measured using the chromogenic substrate ABTS at pH 7.4 [35]. Each 10-mL calibrated flask contained 0.100 g/L cyt *c*, 2.0 mL pH 7.4 B-R buffer, 1.0 mL 1.5 M NaCl and 0–300 mg/L nano-SiO_2 particles. Simultaneously, a series of suspensions were prepared, initially containing 0.025–0.200 g/L cyt *c*, 100 mg/L nano-SiO_2, 2.0 mL pH 7.4 B–R buffer and 1.0 mL 1.5 M NaCl. These suspensions were put into a water bath and incubated at 37 °C for 24 h with magnetic stirring (500 rpm). Free cyt *c* and cyt *c*-SiO_2 were prepared, then fresh ABTS solution was added. Hydrogen peroxide was added to give a final mixture (25 mM ABTS, 120 mM hydrogen peroxide) for incubating native free cyt *c* and cyt *c* adsorbed on nano-SiO_2. After the H_2O_2 was added, the samples were immediately transferred to a UV–vis spectrophotometer and the absorbance increase at 415 nm was recorded for 5 min. The initial reaction rate and the peroxidase activity for each sample were then normalized against the concentration of cyt *c*.

DNase II activity was assayed by the single radial enzyme diffusion (SRED) method [36]. A series of suspensions were prepared, initially containing 0–1000 mg/L nano-SiO_2, 0.600 mg/L DNase II, 2.0 mL pH 7.4 B–R buffer and 1.0 mL 1.5 M NaCl. The suspensions were incubated in a water bath and incubated at 37 °C for 24 h with magnetic stirring at 500 rpm. In brief, 5 μL of sample was poured into a well on a 1% agarose gel plate (containing 20 mM EDTA, 0.1 M sodium acetate buffer pH 7.4, 5 mg/L DNA and 50 mg/L methyl green). After incubation at 37 °C for 24 h, the radius (rs) of the dark circle zone produced by degradation of the DNA accompanying radial diffusion of the enzyme from the wells was measured under UV illumination. A calibration curve was constructed by plotting the logarithm of the enzyme activity against the diffusion radius (rs–ro).

3. Results and discussion

3.1. Effect of proteins on properties of SiO_2 particles

The light absorption of the protein-SiO_2 complex suspensions (A) always increased according to the relationship: $A = \varphi\varepsilon^{-2}\lambda^{-\sqrt{\varepsilon}}$ [31] (λ = wavelength, φ = number factor, proportional to particle number and ε = size factor, inversely proportional to particle size) with increasing protein concentration (Fig. S1 a–c). Both φ and ε were calculated by linear regression plots of lg A vs. lg λ (Fig. S1 d–f)

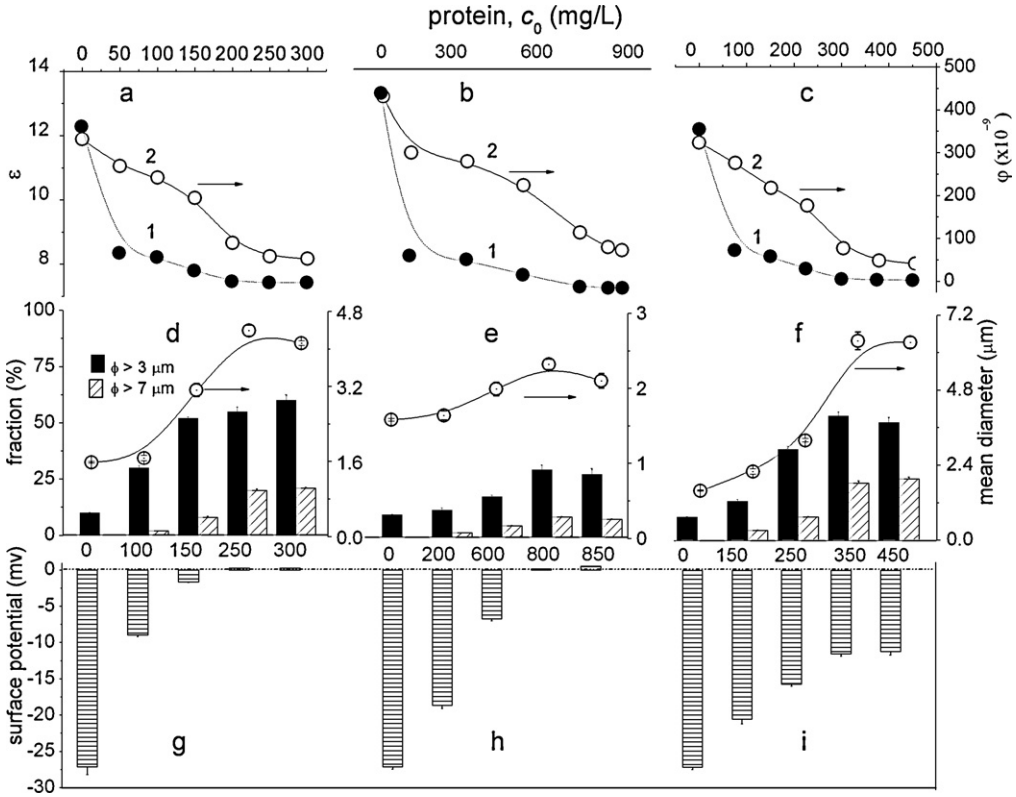

Fig. 1. Variations of ε (curve 1) and φ (2) in the cyt *c*- (a), DNase II- (b), and Hb- SiO_2 (c) suspensions with 150 (a) and 300 (b and c) mg/L nano-SiO_2. The sizes (>3 μm and >7 μm) fraction (d–f) and surface potentials (g–i) of the suspended particles mixed with the proteins (d, g: cyt *c*; e, h: DNase II; and f, i: Hb) at pH 7.4 in 0.15 M NaCl.

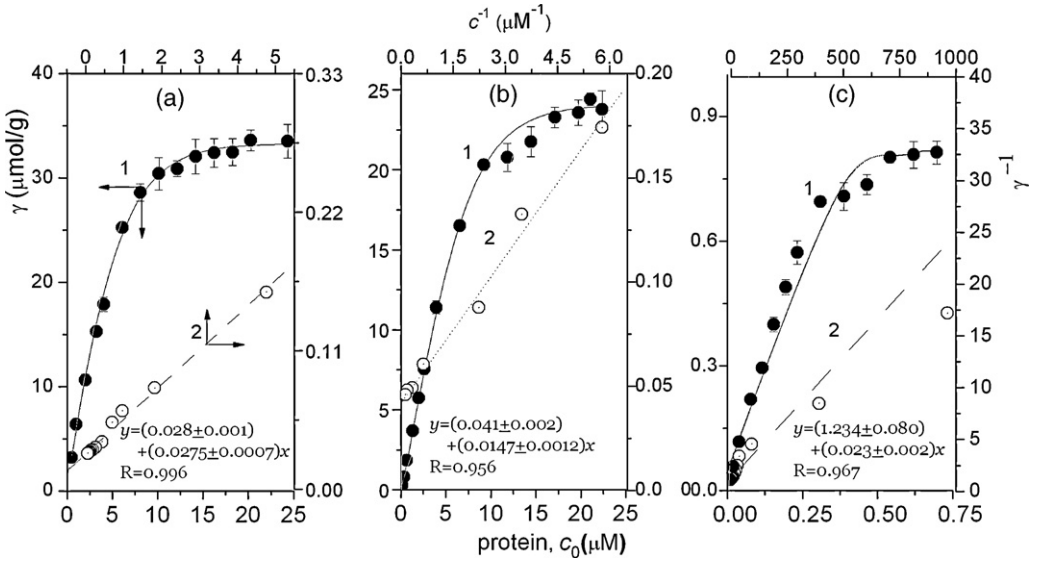

Fig. 2. (1) Variation of γ values of the three functional proteins in the presence of nano-SiO_2. (a) The suspensions contained 150 mg/L SiO_2 and cyt *c* from 6.25 to 300 mg/L (c_0), (b) 300 mg/L SiO_2 and DNase II from 6.25 to 850 mg/L, (c) 300 mg/L SiO_2 and Hb from 6.25 to 450 mg/L. All were at pH 7.4 in 0.15 M NaCl. (2) Plots of c^{-1} vs. γ^{-1} for the above suspensions.

and the changes are shown in Fig. 1a–c. From curves 2, φ (and hence the number of suspended particles) always decreased with increasing protein concentration. From curves 1, the decrease of ε shows that larger particles were formed as soon as protein was added. When the mass ratios of cyt *c*, Hb and DNase II to SiO_2 were less than 0.25, 0.40 and 0.70, respectively, both φ and ε changed markedly. From the size distribution (Fig. 1d–f), the aggregates of SiO_2 particles increased in size with increasing concentrations of cyt *c* from 0 to 250 mg/L, DNase II from 0 to 700 mg/L and Hb from 0 to 400 mg/L. For example, only 10% and 0% of the SiO_2 particles were more than 3

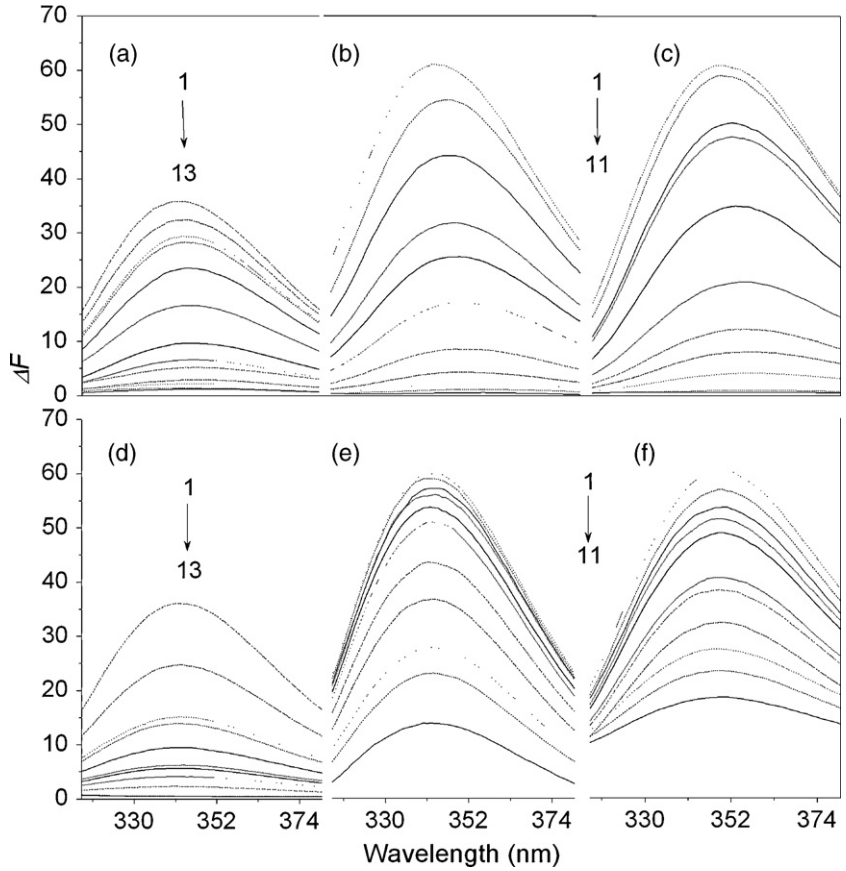

Fig. 3. (a) Fluorescence spectra of nano-SiO_2-cyt *c* suspensions containing 75 mg/L cyt *c* and 0, 50, 100, 150, 200, 250, 300, 400, 500, 600, 700, 800 and 900 mg/L SiO_2 (from curves 1 to 13); (b) same as (a) but containing 350 mg/L DNase II and 0, 10, 30, 50, 75, 100, 150, 200, 250, 300 and 400 mg/L SiO_2 (from curves 1 to 11); (c) same as (a) but containing 100 mg/L Hb and 0, 25, 50, 100, 150, 200, 250, 300, 350, 400 and 500 mg/L SiO_2 (from curves 1 to 11). All the suspensions were at pH 7.4 in 0.15 M NaCl and were measured against the reagent blank. (d–f) The spectra of the supernatants from the above suspensions.

and 7 μm in diameter, respectively, in the absence of cyt *c* (Fig. 1d), but these values increased to over 60% and 21% in 300 mg/L cyt *c*. Mean particle size, initially 4.12 μm, increased 2.6-fold when the cyt *c* concentration exceeded 250 mg/L. Thus, cyt *c* adsorption may approach saturation, as confirmed by Fig. 1a. Using the same method, 800 mg/L DNase II and 300 mg/L Hb both saturated the SiO_2 particle surface (Fig. 1e–f). These results showed that the proteins caused aggregation of the SiO_2 particles, perhaps playing a bridging role. This was confirmed by the SEM images (Fig. S2). The SiO_2-only particles readily formed irregular self-aggregates with sharp edges and corners, but the particles adhered into coralloids in the presence of cyt *c*, DNase II or Hb (Fig. S2). Proteins therefore appear to prevent the self-aggregation of nano-SiO_2 particles and may bridge between them.

The changes in SiO_2 surface potential (Fig. 1g–i) showed that the SiO_2 particle surface carried a number of negative charges because its isoelectric point was pH 2 [37,38]. As is well known, cyt *c* consists of 104 of amino acid residues, 24 of which are basic (Lys, His and Arg) and 12 acidic (Asp and Glu). Because the dissociation constant (pK_R) of His residue is 6.0, it charges negatively at pH 7.4. From the change in column height in Fig. 1g, the ζ-potential of the SiO_2-cyt *c* aggregates decreased from −27.12 mV to +0.23 mV when cyt *c* was added to 300 mg/L. As in the interaction of lysozyme with nano-TiO_2 [39], positive/negative charge attraction induced cyt *c* binding to the nano-SiO_2 particles. The 21 Lys (5, 7, 8, 13, 22, 25, 27, 39, 53, 55, 60, 72, 73, 79, 86, 87, 88, 99 and 100) and Arg (38 and 91) side chains might have bound directly to the SiO_2 surfaces at pH 7.4. Similarly, Fig. 1h shows that the ζ-potential was neutralized when the DNase II concentration exceeded 800 mg/L. In DNase II, 44 of the 259 amino acid residues are basic (Lys 55, 56, 62, 79, 91, 94, 97, 119, 131, 159, 174, 175, 193, 202, 226, 231, 234, 250 and 267, Arg (29, 66, 110, 120, 141, 198, 203, 224, 227, 260 and 261) and 45 are acidic. Fig. 1i shows that increasing Hb concentration gradually decreases the ζ-potential of the particles. Hb consists of four peptide chains with 572 amino acid residues, 62 of which form positive charges: Lys 7, 11, 16, 40, 56, 61, 68, 90, 99, 127 and 139, and Arg 31, 92 and 141 on chain a; Lys 7, 16, 18, 58, 65, 75, 81, 94, 103, 119 and 131, and Arg 29, 39, 115 and 143 on chain b; LYS7, 11, 16, 40, 56, 61, 68, 90, 99, 127 and 139, and ARG31, 92 and 141 on chain *c*; and Lys 7, 16, 18, 58, 60, 64, 65, 75, 81, 94, 103, 119 and 131, and Arg 29, 39, 115 and 143 on chain d. In contrast to cyt *c* and DNase II, Hb has a net negative charge at pH 7.4. The isoelectric points are: cyt *c* 10.6 [40], DNase II 7.7 [41] and Hb 6.8 [42]. The ζ-potential of the SiO_2-Hb aggregate therefore approaches a constant value of −11 mV irrespective of Hb concentration (Fig. 1i).

3.2. Langmuir aggregation of proteins on nano-SiO_2 particles

From curves 1 in Fig. 2, the number (γ) of proteins bound to SiO_2 particles increased with increasing cyt *c*, DNase II and Hb concentration. All γ values approached constant maxima when the protein concentrations (c_0) were more than 0.250 (cyt *c*), 0.85 (DNase II) and 0.450 (Hb) g/L. The Langmuir isotherm equation: $1/\gamma = 1/N + 1/KNc_L$ (γ = the protein binding number, N = the saturation number of a protein and K = the stability constant of an aggregate) [43] was used to fit the above data as curves 1 in Fig. 2. Plots of γ^{-1} vs. $c_L{}^{-1}$ were clearly linear, so all the interactions obeyed the monolayer adsorption isotherm. From the intercepts of lines 2 in Fig. 2, the N values of cyt *c*, DNase II and Hb were 42 ± 5, 24 ± 2 and 1.1 ± 0.1 μmol/g SiO_2, respectively. Considered in conjunction with HSA and BSA binding to nano-TiO_2 [37,44], the results indicate that N decreases with increasing peptide chain length. This indicates that the saturation of binding depends on both the length and the steric effect of the peptide chain. From the slopes, the K values of cyt *c*-, DNase II- and Hb-SiO_2 aggregates were 6.15×10^5, 1.79×10^6 and 2.6×10^7 M^{-1}, respectively.

Table 1
Change of the secondary conformation factors of cyt *c*, Dnase II and Hb in nano-SiO_2 particles presence.

SiO_2 added[a]	cyt *c*				Dnase II				Hb			
	α-helix	β-sheet	β-turn	Random coli	α-helix	β-sheet	β-turn	Random coli	α-helix	β-sheet	β-turn	Random coli
A0	33.70 ± 1.52	0.00 ± 0	31.60 ± 0.85	34.70 ± 1.60	15.70 ± 0.33	33.00 ± 1.06	19.20 ± 0.86	32.10 ± 0.39	42.60 ± 0.47	19.60 ± 0.74	15.70 ± 0.75	22.00 ± 0.42
A1	33.60 ± 1.04	1.90 ± 0.06	31.10 ± 1.56	33.40 ± 1.14	17.30 ± 0.75	28.00 ± 0.73	21.80 ± 0.74	32.90 ± 0.49	47.10 ± 1.60	17.20 ± 0.86	17.30 ± 0.26	18.40 ± 0.31
A2	29.70 ± 1.13	7.90 ± 0.21	29.30 ± 0.56	33.10 ± 0.53	28.20 ± 0.51	2.00 ± 0.10	31.30 ± 1.31	38.50 ± 0.46	51.10 ± 1.17	9.20 ± 0.14	19.40 ± 0.23	20.20 ± 0.38
A3	24.80 ± 1.19	14.50 ± 0.64	27.50 ± 0.88	33.20 ± 1.03	29.90 ± 1.05	0.00 ± 0	30.10 ± 0.33	40.00 ± 1.60	56.80 ± 0.74	0.00 ± 0	25.10 ± 1.23	18.10 ± 0.51

[a] A0: The absence of SiO_2; from A1 to A3: 100, 200 and 300 mg/L SiO_2 added in cyt *c* system and 150, 300 and 500 mg/L SiO_2 added in Dnase II and Hb systems. All are three replicated determinations.

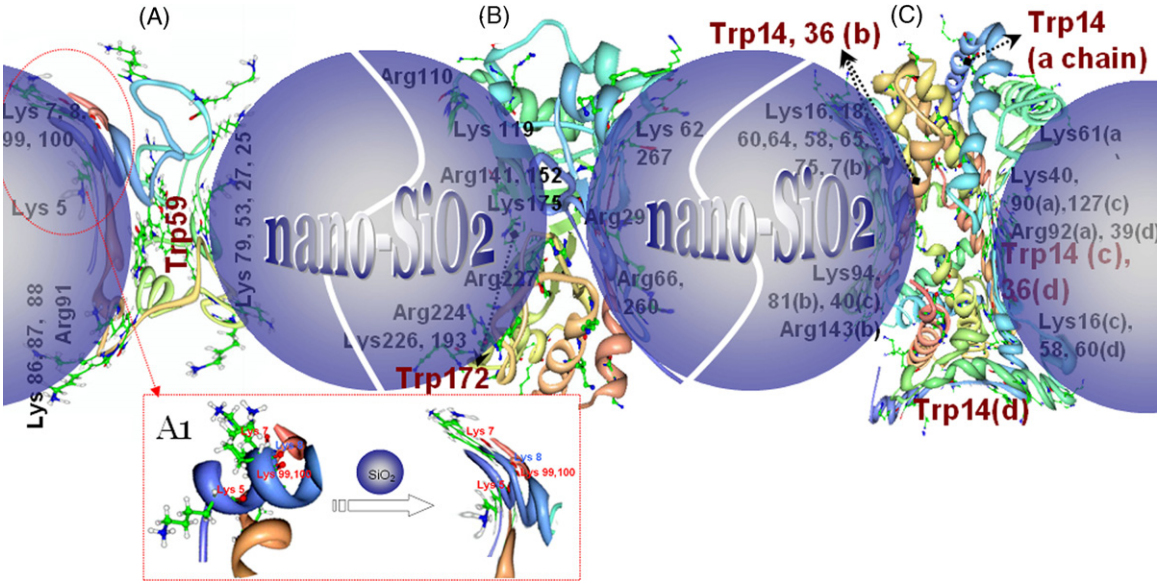

Fig. 4. Cartoon illustrating the possible protein binding sites on SiO_2 particles. (A) cyt *c*, (B) DNase II and (C) Hb. Positive–negative charge attraction pulled the peptide chain binding on the particle surface and N–H···O and O–H···O hydrogen bonds formed. Twisting and transmutation of the peptide chain are illustrated intuitively and the possible positive and Trp residues binding to SiO_2 surface are marked. A1-schematic illustration of the interaction of cyt *c* with nano-SiO_2.

K increases with increasing numbers of Lys and Arg residues, i.e. the number of possible contacts with the SiO_2 surface. In addition to the positively and negatively charged residues, proteins also contain polar residues e.g. Thr, Tyr, Asn, Gln, Cys and SER. In fact, when the positively charged side groups in a protein bind to SiO_2, hydrogen bonds will form between SiO_2 and these polar groups in the N–H···O and O–H···O form [39]. For example, the polar residues of cyt *c*: Thr 89, 63, 58, 49, 47 and 28, Tyr 74, Asn 103, Gln 12, 16 and 42, and Cys 14 and 17, which are located near the positively charged residues, will also bind to SiO_2 via hydrogen bonds. The *N* values of the three proteins adsorbed to nano-SiO_2 (Fig. 2) are much higher than that of polyethylene oxide adsorbed to silica [45]. This strongly suggests that electrostatic attraction is the main interaction force. Thus, the proteins were adsorbed to the nano-SiO_2 particles by a combination of charge attraction and hydrogen bonding, i.e. the stability (*K*) of a protein-SiO_2 aggregate depends on such a combination of interactions.

3.3. Estimation of binding sites from the fluorescence change

The binding sites of the functional proteins may be estimated from the changes in fluorescence spectra. From the curves in Fig. 3a–c, SiO_2 quenched the fluorescence of the proteins and also caused a red shift of the spectra, which may be attributed to light adsorption and scatting by the SiO_2 particles. By comparing the curves in Fig. 3a with those in Fig. 3d, the fluorescence intensity of the cyt *c*-SiO_2 suspension is always greater than that of the corresponding supernatant without SiO_2 particles. For example, the fluorescence of free cyt *c* decreased by 83% (curve 3 in Fig. 3d) but that of the suspension containing 250 mg/L nano-SiO_2 decreased by 53% (curve 3 in Fig. 3a). This showed that cyt *c* bound to SiO_2 particles emits fluorescence as well as free cyt *c*. The strongly fluorescent residue Trp59 in cyt *c* may not connect with SiO_2, as illustrated in Fig. 4a. Trp59 is distant from the positively charged residues. In contrast, the fluorescence intensities of the DNase II–SiO_2 and Hb–SiO_2 suspensions (Fig. 3b and c) were always less than those of the cor-

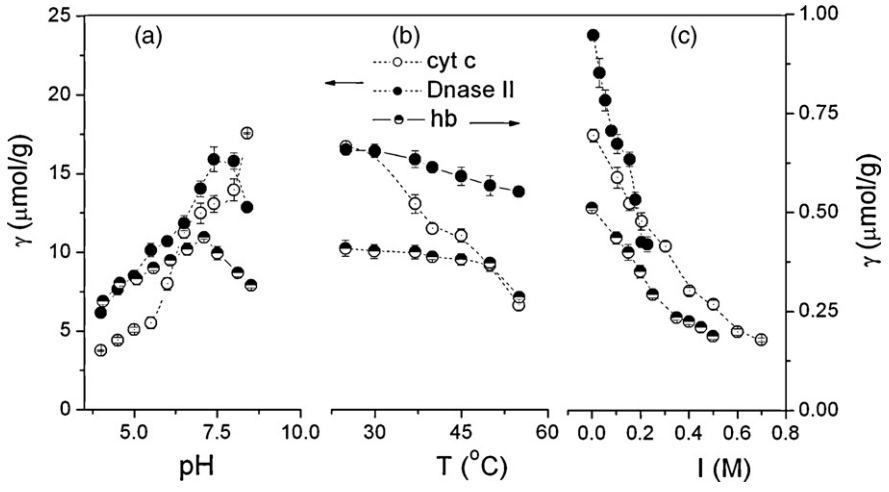

Fig. 5. Effects of pH (a), temperature (b) and electrolyte (c) on γ values of the three functional proteins. (1) 75 mg/L cyt *c* and 150 mg/L nano-SiO_2 particles (○); (2) 350 mg/L DNase II and 300 mg/L nano-SiO_2 particles (●); (3) 100 mg/L Hb and 300 mg/L nano-SiO_2 particles (◓).

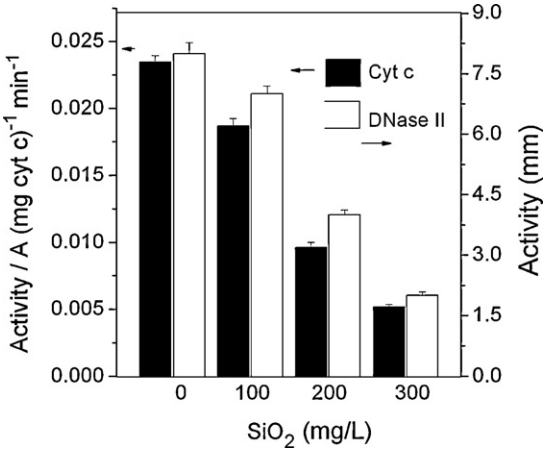

Fig. 6. Changes in cyt *c* peroxidase (■) and Dnase II (□) activities, where the suspensions contained 100 mg/L cyt *c* (■), 0.600 mg/L Dnase II (□) and nano-SiO_2 particles from 0 to 300 mg/L at pH 7.4 in 0.15 M NaCl.

responding supernatants (Fig. 3e and f), i.e. DNase II and Hb bound to SiO_2 particles did not emit fluorescene. This may be attributed to the fact that the Trp side groups of DNase II (Trp172) and Hb (Trp 14, 36) are located near the positively charged residues. When the Lys and Arg residues were bound to SiO_2, the Trp side group was pressed, pulled and then pasted on to the SiO_2 particles via an N–H···O hydrogen bond (Fig. 4b and c). Thus, the fluorescent group was covered and its structure changed.

3.4. Identification of the binding subdomain from change of protein conformation

CD is often used to characterize protein secondary structures (β-pleated sheet, β-turn, α-helix and random coil). From the CD spectra of the three functional proteins (Fig. S3), the nano-SiO_2 particles had a dramatic effect on their secondary structures. As in the adsorption of human carbonic anhydrase to silica nanoparticles [39,46], the fractions of α-helix and β-turn in cyt *c* decreased markedly but the β-sheet fraction increased with increasing SiO_2 particle numbers. For example, the α-helix decreased from 33.7% in absence of SiO_2 to 24.8% in 300 mg/L SiO_2 and the β-sheet increased from 0% to 14.5% (Table 1). The α-helix area of cyt *c* binds directly to the SiO_2 particles and the press and pull interaction breaks the original hydrogen bonds in the α-helix, changing the spiral peptide chain into a sheet-like conformation (Fig. 4a). As in the binding of small organic substance to lysozyme [34], the fractions of α-helix and β-turn in DNase II and Hb increased with increasing SiO_2 particle numbers but the fraction of β-sheet decreased (Fig. S3b and c): the α-helical content of DNase II increased from 15.7% in the absence of SiO_2 to 29.9% in 500 mg/L SiO_2 but the β-sheet decreased from 33.0% to 0 (Table 1). This indicates that the β-pleated sheet areas of DNase II and Hb bound directly to the SiO_2 particles and the press and pull interactions twisted the sheets (Fig. 4b and c). Thus, a helix-like structure may have formed. Such a conformation change necessarily altered the microenvironment of the Trp groups and caused dramatic fluorescence quenching (Fig. 3b and c).

3.5. Effects of pH, ionic strength and temperature

The effects of pH, electrolyte content and temperature on the interactions of the three proteins with nano-SiO_2 particles are shown in Fig. 5. As in the interaction of BSA with nano-TiO_2 particles [44], γ increased as the pH rose from 4.0 to 7.4 (Fig. 5a). Although the SiO_2 particle ζ-potential increased at pHs above 8 (Fig. S4), the Lys and Arg residues were less positively charged, so the charge attraction between protein and SiO_2 particle weakened and γ decreased. From the curves in Fig. 5b, γ decreased as the temperature rose from 25 to 55 °C, presumably because the protein conformation expanded at higher temperatures. From the curves in Fig. 5c, γ decreased sharply with increasing ionic strength. This confirms that electrostatic attraction is the main interaction force between the protein and the nano-SiO_2 particle. The double electric layer on the nano-SiO_2 particles adsorbed Na^+ so the positively charged side groups of proteins were repelled. The induction, orientation and dispersion forces between proteins and nano-SiO_2 become stronger in a high salt medium owing to polarization. However, this is different from the adsorption between HSA and nano-TiO_2 [37].

3.6. Effect of nano-SiO_2 particles on the activities of cyt c and DNase II

The structure of a protein corresponds to its function so structural change may alter normal physiological activity [47]. The

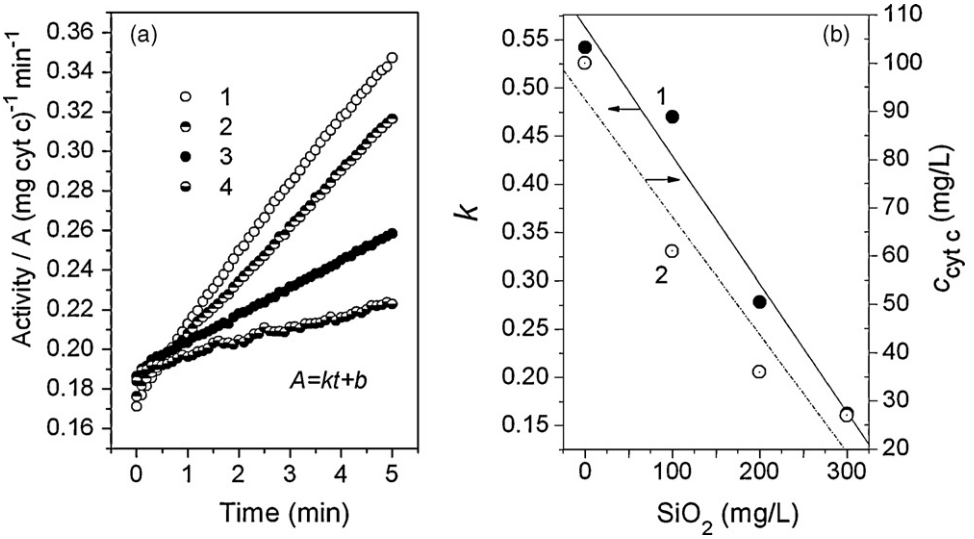

Fig. 7. (a) Absorbance spectra of nano-SiO_2-cyt *c* suspensions initially containing 0.100 mg/L cyt *c*, SiO_2 from 0, 100 and 200 to 300 mg/L (from curves 1 to 4), 25 mM ABTS, 120 mM hydrogen peroxide, and 0.15 M NaCl at pH 7.4, all measured against the reagent blank. (b) Correlation between the activity rate constant (k = dA/dt) (line 1) and free cyt *c* (ccyt *c*) (line 2) and SiO_2 content.

function of cyt *c* is to transport electrons from cyt c_1 to cytochrome oxidase, a shuttle connecting two respiratory chain energy transducers [48]. DNase II is important for DNA fragmentation and degradation during cell death and contributes to the degradation of exogenous DNA ingested by phagocytosis [49]. Nano-SiO_2 particles have a marked effect on the protein structure as described above. The activities of cyt *c* and DNase II were determined in nano-SiO_2 media (Fig. 6). Both proteins approached 75% inactivation in 300 mg/L SiO_2 media. This is attributable to the positive charge on the active site e.g. His residue [50] at pH 5.0. Thus, it will bind to the nano-SiO_2 particle surface and then be covered and hence inactivated.

The dynamic change of cyt *c* activity in SiO_2 (Fig. 7 a) corresponded to the linear equation: $A = kt + b$, where t is the reaction time (min), k, i.e. dA/dt the activity rate constant and b the regression constant. From Fig. 7b, plots of k vs. c_{SiO_2} were linear and the activity rate constant was inversely proportional to the SiO_2 content. Because line 2 is almost parallel to line 1, cyt *c* bound to SiO_2 particles had no activity, i.e. free cyt *c* alone remained active. Nano-SiO_2 particles inactivate cyt *c* but not cause no synergistic effect, in contrast to other reports [35].

4. Conclusions

The adsorption of three functional proteins to nano-SiO_2 obeyed the Langmuir isotherm model. Charge attraction induced protein binding to nano-SiO_2 particles by positive/negative attraction and hydrogen bonds. The acidities and ion strengths of the media markedly affected the interactions. The protein binding area and binding site were estimated by ζ-potential, fluorescence and CD measurements and then the binding model was inferred. Nano-SiO_2 particles changed the secondary conformations of proteins by twisting and pulling the peptide chains, seriously affecting their activity. From the dynamic change in cyt *c* activity, nano-SiO_2 particles inactivated the protein but caused no synergistic effect.

Acknowledgements

This work was supported financially by the National 973 Project of China (Grant No. 2010CB912604) and the State Key Laboratory Foundation of China Science and Technology Ministry (PCRRY09008).

Appendix A. Supplementary data

Supplementary data associated with this article can be found, in the online version, at doi:10.1016/j.jhazmat.2010.04.042.

References

[1] A. Nel, T. Xia, L. Madler, N. Li, Toxic potential of materials at the nanolevel, Science 311 (2006) 622–627.
[2] W. Su, S.S. Wei, S.Q. Hu, J.X. Tang, Preparation of TiO_2/Ag colloids with ultraviolet resistance and antibacterial property using short chain polyethylene glycol, J. Hazard. Mater. 172 (2009) 716–720.
[3] H.J. Zhu, Y.F. Jia, X. Wu, H. Wang, Removal of arsenic from water by supported nano zero-valent iron on activated carbon, J. Hazard. Mater. 172 (2009) 1591–1596.
[4] C.S. Sundaram, N. Viswanathan, S. Meenakshi, Fluoride sorption by nano-hydroxyapatite/chitin composite, J. Hazard. Mater. 172 (2009) 147–151.
[5] L. Zhang, N. Liu, L.J. Yang, Q. Lin, Sorption behavior of nano-TiO_2 for the removal of selenium ions from aqueous solution, J. Hazard. Mater. 170 (2009) 1197–1203.
[6] M. Rivero-Huguet, W.D. Marshall, Reduction of hexavalent chromium mediated by micro- and nano-sized mixed metallic particles, J. Hazard. Mater. 169 (2009) 1081–1087.
[7] Y.J. Wu, J.H. Zhang, Y.F. Tong, X.H. Xu, Chromium (VI) reduction in aqueous solutions by Fe3O4-stabilized Fe-0 nanoparticles, J. Hazard. Mater. 172 (2009) 1640–1645.
[8] K. Donaldson, V. Stone, A. Seaton, W. MacNee, Ambient particle inhalation and the cardiovascular system: potential mechanisms, in: Workshop on Inhaled Environmental/Occupational Irritants and Allergens – Mechanisms of Cardiovascular and Systemic Responses, Scottsdale, Arizona, 2000, 2000, pp. 523–527.
[9] R. Dunford, A. Salinaro, L.Z. Cai, N. Serpone, S. Horikoshi, H. Hidaka, J. Knowland, Chemical oxidation and DNA damage catalysed by inorganic sunscreen ingredients, FEBS Lett. 418 (1997) 87–90.
[10] M. Fenech, The in vitro micronucleus technique, Mutat. Res. -Fund. Mol. Mech. 455 (2000) 81–95.
[11] W.G. Kreyling, M. Semmler-Behnke, W. Moller, Health implications of nanoparticles, J. Nanopart. Res. 8 (2006) 543–562.
[12] J. Ovrevik, M. Lag, J.A. Holme, P.E. Schwarze, M. Refsnes, Cytokine and chemokine expression patterns in lung epithelial cells exposed to components characteristic of particulate air pollution, Toxicology 259 (2009) 46–53.
[13] J. Ovrevik, M. Refsnes, P. Schwarze, M. Lag, The ability of oxidative stress to mimic quartz-induced chemokine responses is lung cell line-dependent, Toxicol. Lett. 181 (2008) 75–80.
[14] A.J. Di Pasqua, K.K. Sharma, Y.L. Shi, B.B. Toms, W. Ouellette, J.C. Dabrowiak, T. Asefa, Cytotoxicity of mesoporous silica nanomaterials, J. Inorg. Biochem. 102 (2008) 1416–1423.
[15] W.S. Lin, Y.W. Huang, X.D. Zhou, Y.F. Ma, In vitro toxicity of silica nanoparticles in human lung cancer cells, Toxicol. Appl. Pharm. 217 (2006) 252–259.
[16] L. De Boni, A.A. Andrade, L. Misoguti, S.C. Zilio, C.R. Mendonca, Excited-state absorption spectroscopy in oxidized Cytochrome c, Opt. Mater. 32 (2010) 526–529.
[17] L. De Boni, D.S. Correa, F.J. Pavinatto, D.S. dos Santos, C.R. Mendonca, Excited state absorption spectrum of chlorophyll a obtained with white-light continuum, J. Chem. Phys. 126 (2007) 4.
[18] J.H. Kang, Modification and inactivation of human ceruloplasmin by oxidized DOPA, Bull. Korean Chem. Soc. 25 (2004) 625–628.
[19] N.H. Kim, M.S. Jeong, S.Y. Choi, J.H. Kang, Peroxidase activity of cytochrome c, Bull. Korean. Chem. Soc. 25 (2004) 1889–1892.
[20] M.A. Barry, A. Eastman, Identification of deoxyribonuclease II as an endonuclease involved in apoptosis, Arch. Biochem. Biophys. 300 (1993) 440–450.
[21] G. Bernardi, A. Bernardi, A. Chersi, Studies on acid hydrolases. I. A procedure for the preparation of acid deoxyribonuclease and other acid hydrolases, Biochim. Biophys. Acta 129 (1966) 1–11.
[22] C.C. Wang, S.C. Lu, H.L. Chen, T.H. Liao, Porcine spleen deoxyribonuclease II - Covalent structure, cDNA sequence, molecular cloning, and gene expression, J. Biol. Chem. 273 (1998) 17192–17198.
[23] M. Arends, R. Morris, A. Wyllie, Apoptosis, The role of the endnuclease, Am. J. Pathol. 136 (1990) 593–608.
[24] Y.Q. Wang, H.M. Zhang, R.H. Wang, Investigation of the interaction between colloidal TiO_2 and bovine hemoglobin using spectral methods, Colloids Surf. B 65 (2008) 190–196.
[25] H. Larsericsdotter, S. Oscarsson, J. Buijs, Structure, stability, and orientation of BSA adsorbed to silica, J. Colloid Interface Sci. 289 (2005) 26–35.
[26] W. Norde, C.E. Giacomelli, BSA structural changes during homomolecular exchange between the adsorbed and the dissolved states, in: 2nd International Symposium on Industrial Proteins + Noordwijkerhout, Netherlands, 1999, pp. 259–268.
[27] A.D. Roddick-Lanzilotta, P.A. Connor, A.J. McQuillan, An in situ infrared spectroscopic study of the adsorption of lysine to TiO_2 from an aqueous solution, Langmuir 14 (1998) 6479–6484.
[28] H. Larsericsdotter, S. Oscarsson, J. Buijs, Thermodynamic analysis of proteins adsorbed on silica particles: electrostatic effects, J. Colloid Interface Sci. 237 (2001) 98–103.
[29] M. Horie, K. Nishio, K. Fujita, S. Endoh, A. Miyauchi, Y. Saito, H. Iwahashi, K. Yamamoto, H. Murayama, H. Nakano, N. Nanashima, E. Niki, Y. Yoshida, Protein adsorption of ultrafine metal oxide and its influence on cytotoxicity toward cultured cells, Chem. Res. Toxicol. 22 (2009) 543–553.
[30] T. Nezu, T. Masuyama, K. Sasaki, S. Saitoh, M. Taira, Y. Araki, Effect of pH and addition of salt on the adsorption behavior of lysozyme on gold, silica, and titania surfaces observed by quartz crystal microbalance with dissipation monitoring, Dent. Mater. J. 27 (2008) 573–580.
[31] H.W. Gao, Establishement of SS absorption in suspension liquid, Asian J. Chem. 11 (1999) 1556–1558.
[32] H.G. Zhu, R. Srivastava, J.Q. Brown, M.J. McShane, Combined physical and chemical immobilization of glucose oxidase in alginate microspheres improves stability of encapsulation and activity, Bioconjugate Chem. 16 (2005) 1451–1458.
[33] Z.G. Peng, K. Hidajat, M.S. Uddin, Adsorption and desorption of lysozyme on nano-sized magnetic particles and its conformational changes, Colloids Surf. B 35 (2004) 169–174.
[34] F.F. Chen, Y.N. Tang, S.L. Wang, H.W. Gao, Binding of brilliant red compound to lysozyme: insights into the enzyme toxicity of water-soluble aromatic chemicals, Amino Acids 36 (2009) 399–407.
[35] W. Shang, J.H. Nuffer, V.A. Muniz-Papandrea, W. Colon, R.W. Siegel, J.S. Dordick, Cytochrome c on silica nanoparticles: influence of nanoparticle size on protein structure, stability, and activity, Small 5 (2009) 470–476.
[36] D.L. Horney, D.A. Webster, Deoxyribonuclease: a sensitive assay using radial diffusion in agarose containing methyl green-DNA complex, Biochim. Biophys. Acta 247 (1971) 54–61.
[37] F.Y. Oliva, L.B. Avalle, O.R. Camara, C.P. De Pauli, Adsorption of human serum albumin (HSA) onto colloidal TiO_2 particles, Part I, J. Colloid Interface Sci. 261 (2003) 299–311.

[38] C. Mohr, H. Hofmeister, M. Lucas, P. Claus, Gold catalysts for the partial hydrogenation of acrolein, Chem. Ing. Tech. 71 (1999) 869–873.
[39] Z. Xu, X.W. Liu, Y.S. Ma, H.W. Gao, Interaction of nano-TiO_2 with lysozyme: insights into the enzyme toxicity of nanosized particles, Environ. Sci. Pollut. R 17 (2010) 798–806.
[40] S. Emir, R. Say, H. Yavuz, A. Denizli, A new metal chelate affinity adsorbent for Cytochrome c, Biotechnol. Progr. 20 (2004) 223–228.
[41] M.Q. Ye, Z. Hu, Y. Fan, L. He, F.B. Xia, G.L. Zou, Pnrification and characterization of an acid deoxyribonuclease from the cultured mycelia of Cordyceps sinensis, J. Biochem. Mol. Biol. 37 (2004) 466–473.
[42] A. Uysal, G. Demirel, E. Turan, T. Caykara, Hemoglobin recognition of molecularly imprinted hydrogels prepared at different pHs, Anal. Chim. Acta 625 (2008) 110–115.
[43] S. Fukuzaki, H. Urano, K. Nagata, Adsorption of bovine serum albumin onto metal oxide surfaces, J. Ferment. Bioeng. 81 (1996) 163–167.
[44] C.E. Giacomelli, M.J. Avena, C.P. DePauli, Adsorption of bovine serum albumin onto TiO_2 particles, J. Colloid Interface Sci. 188 (1997) 387–395.
[45] B. Wind, E. Killmann, Adsorption of polyethylene oxide on surface modified silica stability of bare and covered particles in suspension, Colloid Polym. Sci. 276 (1998) 903–912.
[46] M. Lundqvist, I. Sethson, B.H. Jonsson, Protein adsorption onto silica nanoparticles: conformational changes depend on the particles' curvature and the protein stability, Langmuir 20 (2004) 10639–10647.
[47] H.Y. Hu, G.J. Xu, Structural transformation of proteins, Prog. Biochem. Biophys. 26 (1999) 9–12.
[48] V.P. Skulachev, Cytochrome c in the apoptotic and antioxidant cascades, FEBS Lett. 423 (1998) 275–280.
[49] C.J. Evans, R.J. Aguilera, DNase II: genes, enzymes and function, Gene 322 (2003) 1–15.
[50] A. Watanabe, H. Nagai, Y. Nagashima, K. Shiomi, Structural characterization of plancitoxin I, a deoxyribonuclease II-like lethal factor from the crown-of-thorns starfish Acanthaster planci, by expression in Chinese hamster ovary cells, Fish. Sci. 75 (2009) 225–231.